

Circular polarization in pulsar radio emission due to intrinsically relativistic effects

D. B. Melrose^{*} and Q. Luo

School of Physics, University of Sydney, NSW 2006, Australia

Accepted 2004 May 2. Received 2004 February 11; in original form 2003 October 29

ABSTRACT

Observations of single pulses imply that the circular polarization (CP) at a fixed pulsar phase, in some pulsars, can be large and variable from pulse to pulse. In many cases the variations can include changes in the handedness at a fixed phase. Possible explanations for the variable CP are sought in terms of elliptical polarization of the natural wave modes. The pulsar plasma is assumed to be a highly relativistically streaming, one-dimensional, strongly magnetized, electron–positron gas with a net charge density and intrinsically relativistic random motions in its rest frame. It is shown that in such a plasma the polarization of the natural modes includes two regimes where intrinsically relativistic effects determine the CP. One regime arises from aberration causing a small cone of CP about the backward (anti-streaming) direction in the rest frame to expand into the forward hemisphere in the pulsar frame. This mechanism can lead to significant CP at relatively high frequencies. The other mechanism arises from the intrinsically relativistic random motions, which allow a new regime of CP that has no counterpart in a cold plasma; however, for typical parameters this mechanism is effective only at frequencies higher than is consistent with our neglect of the cyclotron resonance. It is suggested that the explanation for the observed CP requires that the CP arise as a propagation effect, and be determined by the properties of the wave modes at a polarization limiting region.

Key words: plasmas – polarization – radiation mechanisms: non-thermal – pulsars: general.

1 INTRODUCTION

The characteristics of the circular polarization (CP) of pulsar radio emission are well established for the time-integrated pulse profile (Radhakrishnan & Rankin 1990; Han et al. 1998). The CP is typically low, that is, the ratio of the magnitudes of Stokes V to Stokes I is small in magnitude, usually no more than a few per cent. There are, however, some notable exceptions. First, a small fraction of pulsars show a substantial increase in CP at high frequencies (von Hoensbroech & Lesch 1999). Secondly, recent observations of the CP in single pulses (Karastergiou et al. 2001, 2002; Karastergiou, Johnston & Kramer 2003a; Karastergiou et al. 2003b) support and clarify much earlier reports (Ekers & Moffat 1968; Clark & Smith 1969; Lyne, Smith & Graham 1971) of high CP that varies from pulse to pulse. Low average CP, at a given pulsar phase, can result from much higher intrinsic CP that varies from pulse to pulse with a statistical distribution that includes both signs of V , so that the average of V is much smaller than the average of $|V|$ (Karastergiou et al. 2003b). Another feature of the CP applies especially to pulsars where there is evidence for flips in the linear polarization (Stinebring et al. 1984; McKinnon & Stinebring 2000) between two orthogo-

nal modes (OMs), generally referred to as orthogonally polarized modes in the observational literature. The data are generally consistent with the CP reversing sign when a flip between OMs occurs, especially at low frequencies, implying that the OMs are elliptically polarized in general.

The possible explanations for the CP can be divided into three classes. First, the CP is assumed to be intrinsic to the emission mechanism. Secondly, the emission mechanism is assumed to favour one natural mode of the pulsar plasma over the other, and the escaping radiation has the polarization of this preferred mode. Thirdly, the polarization characteristics are assumed to develop as a propagation effect. There are strong arguments against the first two possibilities. The third possibility is favoured by data on OMs that provide evidence for the pulsar emission separating into the two orthogonally polarized natural wave modes, with the rays in these two modes propagating along significantly different paths in the birefringent plasma (Barnard & Arons 1986; Lyubarskii & Petrova 1998; Petrova 2002). The observed polarization reflects the properties of the natural wave modes of the pulsar plasma in a polarization limiting region (Budden 1961), beyond which the plasma is ineffective in causing further changes to the polarization of the escaping radiation. With this model, the interpretation of the data on CP depends on the polarization of the natural wave modes of the pulsar plasma at the polarization limiting region, and this must be partially circular.

^{*}E-mail: melrose@physics.usyd.edu.au

Our purpose in this paper is to discuss the elliptical polarization of the natural wave modes of a pulsar plasma and to apply the results to the interpretation of the observed features of CP in pulsars. The relevant polar-cap region of a pulsar magnetosphere is thought to be populated by a highly relativistic, outwardly streaming, electron–positron plasma created in a cascade (Sturrock 1971; Zhang & Harding 2000; Hibschan & Arons 2001; Arendt & Eilek 2002). Dispersion in a pulsar plasma has been investigated extensively (Volokitin, Krasnoselskikh & Machabeli 1985; Lominadze et al. 1986; Arons & Barnard 1986; Gedalin, Melrose & Gruman 1998; Lyutikov 1998; Asseo & Riazuelo 2000), mostly assuming a pure pair plasma, by which we mean a plasma with identical distributions of electrons and positrons. Such a plasma is non-gyrotropic, meaning that the natural modes are strictly linearly polarized with no CP. However, there is necessarily a net charge density, equal to the Goldreich–Julian density, en_{GJ} , in the plasma, and this implies that the plasma is in fact gyrotropic. In the simplest case the gyrotropy is included by allowing the electrons and positrons to have different number densities, described by the ratio, η , of the difference to the sum of the electron and positron number densities. Thus $\eta = -1$ corresponds to a pure electron gas, and $\eta = 0$ to a pure pair plasma. One expects $|\eta| \sim 1/M$ in a pulsar plasma, where M is the multiplicity, that is, the ratio of the density of secondary pairs to primary particles. A general theory, which includes $\eta \neq 0$ and relativistic random and directed motions, is available (Melrose et al. 1999), and is used in the present discussion. However, the general theory is rather cumbersome, and it is useful to develop the ideas using simpler models for the wave dispersion. A simpler model is based on applying a Lorentz transformation to magneto-ionic theory (Melrose & Stoneham 1977; Allen & Melrose 1982), which ignores the random motions of the particles, which are thought to be highly relativistic (Zhang & Harding 2000; Hibschan & Arons 2001; Arendt & Eilek 2002). Such a model has been used more recently to interpret an increase in CP at high frequency (von Hoensbroech & Lesch 1999), and to discuss other features of the wave dispersion in pulsar plasmas (Lyutikov, Blandford & Machabeli 1999).

One particular feature of the data on single pulses suggests that the handedness of a given mode can change randomly, especially at high frequencies, and this seems to require a specific explanation. The statistics of pulse-to-pulse variations of CP include features that may be described by a simple Gaussian model with a mean V and a variance in V such that both signs of V occur, but with unequal probabilities (Karastergiou et al. 2003a,b). There is no evidence that this change in V is due to a flip between the natural modes. Rather, it seems that the CP of a given mode at a given pulsar phase depends on some parameter that can change randomly about its mean from pulse to pulse. A possible explanation in non-stationarity in the pair production process leading to changes is the location or structure of the polarization limiting region, causing random changes in the polarization ellipse from pulse to pulse, including reversals of handedness of CP.

In this paper CP in the natural wave modes in a pulsar plasma is treated through a stepwise generalization. We start with the magneto-ionic theory, which corresponds to a cold electron gas. Frequencies thought relevant to pulsars are in the range $\omega_p \ll \omega \ll \Omega_e$, where ω_p is the plasma frequency and Ω_e is the cyclotron frequency; the magneto-ionic theory then implies that large CP is confined to small forward and backward cones, $\sin \theta \ll 1$. One relevant generalization of magneto-ionic theory for pulsars is to include an admixture of positrons, and this involves allowing $-1 \leq \eta \leq 1$ to be a free parameter (Section 2). The next generalization (Section 3) is to assume that the (cold pair) plasma is streaming relativistically,

and this is achieved by making a Lorentz transformation from the rest frame of the plasma to the pulsar frame in which the plasma is streaming outward with a high Lorentz factor, $\gamma_s \gg 1$. The third generalization (Section 4) is to include relativistic random motions in the rest frame of the plasma, described by the mean Lorentz factor $\langle \gamma \rangle$. The final generalization is to apply a Lorentz transformation so that the plasma has both highly relativistic random motions and a highly relativistic bulk motion. The implication of the results for the interpretation of CP in pulsar radio emission is discussed in Section 5.

2 COLD PLASMA APPROXIMATION

In this section we start with the description of wave polarization in magneto-ionic theory, generalized here to include a mixture of electrons and positrons ($\eta \neq -1$).

2.1 The magneto-ionic waves

In the rest frame of the plasma, the dispersion equation for the magneto-ionic waves is of the form (Budden 1961; Stix 1962) $An^4 - Bn^2 + C = 0$, where n is the refractive index and the coefficients A, B, C depend on ω and θ . The frequency is conventionally incorporated into the magneto-ionic parameters, denoted here as

$$X = \omega_p^2/\omega^2, \quad Y = \Omega_e/\omega, \quad (1)$$

where the plasma frequency, $\omega_p = (e^2 n_e / \epsilon_0 m)^{1/2}$, is defined here in terms of the number density, n_e , of electrons plus positrons, and $\Omega_e = eB/m$ is the cyclotron frequency. It is convenient to rewrite the dispersion equation for $n^2 - 1 + X$, rather than for n^2 . This gives

$$a(n^2 - 1 + X)^2 - b(n^2 - 1 + X) + c = 0, \quad (2)$$

with $a = A, b = B - 2A(1 - X), c = C - B(1 - X) + A(1 - X)^2$. Explicit expressions are

$$\begin{aligned} a &= 1 - \frac{X(1 - Y^2 \cos^2 \theta)}{1 - Y^2}, \\ b &= -\frac{XY^2}{1 - Y^2}(1 + \cos^2 \theta) \\ &\quad + \frac{X^2 Y^2}{(1 - Y^2)^2} [(1 - \eta^2) \sin^2 \theta + 2(1 - Y^2) \cos^2 \theta], \\ c &= -X^2 \frac{(1 - X)Y^2(\eta^2 - Y^2) \cos^2 \theta}{(1 - Y^2)^2}. \end{aligned} \quad (3)$$

The solutions of the quadratic equation (2) give the dispersion relations

$$n^2 = n_{\pm}^2 = 1 - X + [b \pm (b^2 - 4ac)^{1/2}]/2a. \quad (4)$$

The identification of the \pm modes as the ordinary and extraordinary modes of magneto-ionic theory is not important at this stage. (Technically, the ordinary mode is that for which $n^2 \rightarrow 1 - X$ for $\cos \theta \rightarrow 0$.)

2.2 Polarization of the natural modes

The polarization vector for either mode is of the general form

$$\mathbf{e}_{\pm} = \frac{(L_{\pm} \boldsymbol{\kappa} + T_{\pm} \mathbf{t} + i\mathbf{a})}{(L_{\pm}^2 + T_{\pm}^2 + 1)^{1/2}}, \quad (5)$$

with $\boldsymbol{\kappa} = (\sin \theta, 0, \cos \theta)$ the unit vector along the wavevector, and where

$$\mathbf{t} = (\cos \theta, 0, -\sin \theta), \quad \mathbf{a} = (0, 1, 0), \quad (6)$$

span the transverse plane. The parameter T is the axial ratio of the polarization ellipse, with $T = \pm 1$ corresponding to opposite circular polarizations, and $T = 0, \infty$ corresponding to orthogonal linear polarizations. T satisfies the quadratic equation (Melrose 1980, 1986; Melrose & McPhedran 1991)

$$T^2 - RT - 1 = 0, \quad R = \frac{Y \sin^2 \theta}{\eta(1 - X) \cos \theta}. \quad (7)$$

The solutions are

$$T = T_{\pm} = \frac{1}{2} [R \pm (R^2 + 4)^{1/2}]. \quad (8)$$

The polarization ellipses for the two modes are orthogonal, corresponding to $T_+ T_- = -1$.

One may write n_{\pm}^2 and L_{\pm} in terms of T_{\pm} :

$$n^2 = 1 - \frac{XT}{T - \eta Y \cos \theta}, \quad L = \frac{XY \sin \theta}{1 - X} \frac{T}{T - \eta Y \cos \theta}, \quad (9)$$

with the explicit solutions, n_{\pm}^2 and L_{\pm} , for either mode given by substituting $T = T_{\pm}$ from (8) into (9).

2.3 Transition angle

The axial ratio, T , which completely describes the transverse part of the polarization of a natural wave mode, depends only on the parameter R . The degree of linear polarization is $r_l = (T^2 - 1)/(T^2 + 1)$ and the degree of CP is $r_c = 2T/(T^2 + 1)$. The variations of $|r_l|$ and $|r_c|$ for either of the two solutions (8) as a function of R are plotted in Fig. 1. One has $|r_c/r_l| = 2/|R|$ more generally. For $|R| \gg 2$ the degree of CP is $|r_c| \approx 2/|R|$. The degrees of polarization are equal for $|R| = 2$, and it is convenient to define a transition angle, θ_c , corresponding to $|R| = 2$. Then a given mode is approximately circularly polarized in one sense for $\theta \lesssim \theta_c$, approximately linearly polarized for $\theta_c \lesssim \theta \lesssim \pi - \theta_c$, and approximately circularly polarized in the opposite sense for $\pi - \theta_c \lesssim \theta \leq \pi$.

Writing $|R| = r \sin^2 \theta / \cos \theta$, with $r = Y/\eta(1 - X) \approx Y/\eta$, the transition angle satisfies $2 = r \sin^2 \theta_c / \cos \theta_c$, which gives

$$\theta_c = \arccos \left[\frac{(1 + r^2)^{1/2} - 1}{r} \right] \approx \begin{cases} \pi/2 - r & \text{for } r \ll 1, \\ (2/r)^{1/2} & \text{for } r \gg 1. \end{cases} \quad (10)$$

The most familiar case in magneto-ionic theory is high frequencies, $\omega \gg \omega_p, \Omega_e$, implying $|r| \approx \Omega_e/|\eta|\omega \ll 1$, and then the modes are approximately circularly polarized except for a small range of angles $\sim \omega/\Omega_e$ around $\pi/2$. For the case of most relevance to pulsars, $\omega_p \ll \omega \ll \Omega_e$, one has $r \approx \Omega_e/|\eta|\omega \gg 1$, and the polarizations are

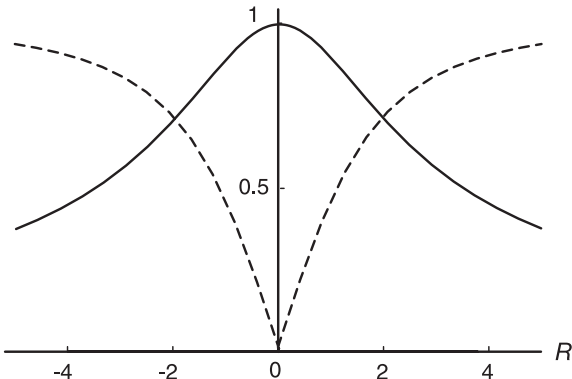


Figure 1. The magnitudes of the degrees of circular (solid line) and linear (dashed line) polarization are plotted for either mode as a function of R .

nearly linear except in small cones about parallel and antiparallel propagation, with the cone angles given approximately by

$$\theta_c = (2\omega|\eta|/\Omega_e)^{1/2}. \quad (11)$$

The size of these cones is proportional to $|\eta|^{1/2} \sim 1/M^{1/2}$, and tends to zero as the net charge density tends to zero. However, the approximation of a pure pair plasma ($\eta \rightarrow 0$) neglects these cones entirely, and this is a poor approximation when highly relativistic streaming is taken into account: aberration expands the backward cone by a large factor, and this can lead to the transformed backward cone filling all solid angles outside a relatively small forward cone (Section 3).

2.4 Weak anisotropy approximation

We are concerned with the wave properties in a relativistically streaming plasma, and these properties cannot be calculated exactly in general. It is straightforward to calculate the wave properties in the streaming plasma by Lorentz-transforming from the rest frame of the plasma only if the longitudinal part of the polarization can be neglected (in both frames). This corresponds to the conditions under which the weak anisotropy approximation is valid (Sazonov & Tsytovich 1968; Melrose 1980). In the weak anisotropy approximation, one assumes the waves to be transverse, and replaces the wave equation by its two-dimensional counterpart, that is, by projecting on to the transverse plane. The refractive index is assumed to be unity, $n^2 = 1$, in the leading approximation.

The weak anisotropy approximation involves neglecting the longitudinal part of the polarization. Conditions under which the longitudinal part can be neglected can be deduced from (9), which implies $L = (1 - n^2)Y \sin \theta / (1 - X)$. It follows that one has $L = 0$ for $n^2 = 1$, and that the neglect of the longitudinal part of the polarization is equivalent to neglecting the difference $1 - n^2$ to first approximation. It follows from (9) that the weak anisotropy limit is not valid near points where the denominator, $T - \eta Y \cos \theta$, vanishes, which can be shown to include plasma resonances. This condition is satisfied in the range $\omega_p \ll \omega \ll \Omega_e$, where one has $X \ll 1$, as there are no resonances in this range.

To lowest order in X , the coefficients a, b, c in (3) are $a = 1$,

$$b = -\frac{XY^2(1 + \cos^2 \theta)}{1 - Y^2}, \quad c = -\frac{X^2Y^2(\eta^2 - Y^2) \cos^2 \theta}{(1 - Y^2)^2}. \quad (12)$$

Then in (4) one has

$$\frac{b \pm (b^2 - 4ac)^{1/2}}{2a} = -\frac{XY[Y(1 + \cos^2 \theta) \pm \Delta]}{2(1 - Y^2)}, \quad (13)$$

with

$$\Delta^2 = Y^2 \sin^4 \theta + \eta^2 \cos^2 \theta. \quad (14)$$

To the lowest order, the quadratic equation (7) for T has

$$R \approx Y \sin^2 \theta / \eta \cos \theta. \quad (15)$$

3 LORENTZ TRANSFORMATION OF MAGNETO-IONIC WAVES

A relatively simple model for the wave properties in a pulsar plasma is obtained by applying a Lorentz transformation to the magneto-ionic waves (Allen & Melrose 1982; Lyutikov et al. 1999). This model takes the bulk relativistic motion of the plasma into account but ignores the relativistic random motion of the particles. The rest frame of the plasma is denoted as the unprimed frame, and the

pulsar or laboratory frame, in which the plasma is streaming relativistically, is denoted as the primed frame. In the laboratory frame the plasma is streaming with velocity $\beta_s c$ and Lorentz factor $\gamma_s = (1 - \beta_s^2)^{-1/2}$ along the 3-axis, which is the direction of the magnetostatic field.

3.1 Lorentz transformation to the pulsar frame

The Lorentz transformation between the primed and unprimed frames gives

$$\begin{aligned}\omega &= \gamma_s \omega' (1 - n' \beta_s \cos \theta'), \\ n \sin \theta &= \frac{n' \sin \theta'}{\gamma_s (1 - n' \beta_s \cos \theta')}, \\ n \cos \theta &= \frac{n' \cos \theta' - \beta_s}{1 - n' \beta_s \cos \theta'}.\end{aligned}\quad (16)$$

Hence, one has

$$\begin{aligned}X &= \frac{\omega_p^2}{\omega^2} \frac{1}{[\gamma_s (1 - \beta_s n' \cos \theta')]^2}, \\ Y &= \frac{\Omega_e}{\omega'} \frac{1}{\gamma_s (1 - \beta_s n' \cos \theta')}.\end{aligned}\quad (17)$$

On substituting (16) and (17) into the explicit expressions for n_{\pm}^2 , these become implicit expressions for

$$n^2 - 1 = \frac{n^2 - 1}{\gamma_s^2 (1 + n \beta_s \cos \theta)^2}, \quad (18)$$

in the primed frame. One cannot solve for explicit expressions for the refractive indices, $n'_{\pm}(\omega', \theta')$, in the primed frame without making approximations.

3.2 Implicit dispersion relations

Formally, the dispersion relations in the primed frame may be written in the form (4), which becomes

$$n_{\pm}^2 = 1 - X' + [b \pm (b^2 - 4ac)^{1/2}]/2a,$$

with $X' = \omega_p^2/\omega'^2$, and where X , Y and θ , which appear in a , b and c , are to be expressed in terms of the primed variables. However, n' appears implicitly in the expressions for a , b and c . An alternative procedure is to write the dispersion relation in terms of the invariant $k^2 = \omega^2/c^2 - |\mathbf{k}|^2$, so that the solutions (4) become

$$k^2 = k_{\pm}^2 = \frac{\omega_p^2}{c^2} \left[1 - \frac{b \pm (b^2 - 4ac)^{1/2}}{2aX} \right]. \quad (19)$$

The dispersion relations in the primed frame are then formally given by (19) with $k^2 = \omega'^2/c^2 - |\mathbf{k}'|^2$ and with a , b and c expressed in terms of the primed variables. However, again the solutions are only implicit.

The weak anisotropy approximation allows one to construct explicit dispersion relations using an iterative procedure. In this limit the refractive indices are close to unity, and $n^2 = 1$ transforms into $n'^2 = 1$ (cf. equation 18). Hence in the primed frame one may set $n' = 1$ in the expressions for a , b and c obtained by inserting (16) into (3) to obtain explicit expressions for $n_{\pm}^2 = 1 - X' + [b \pm (b^2 - 4ac)^{1/2}]/2a$ to lowest order in the iteration. The next step in the iteration is to use these lowest-order solutions for n'_{\pm} in (16) and (3) to find the next-order solutions.

3.3 Transformation of the polarization vectors

Lorentz transformation of the polarization vectors requires several steps. One may regard a polarization vector, \mathbf{e} , as the normalized (to unity) space components of the vector potential of the wave in the temporal gauge, that is, with the scalar potential zero by definition. On making the Lorentz transformation, the transformed polarization vector is not in the temporal gauge, and one must make a gauge transformation to restore the temporal gauge. The transformed vector then needs to be renormalized to unity. Let the transformed polarization vector so constructed, but before the renormalization, be denoted by a subscript 't'.

A general polarization may be separated into longitudinal and transverse parts (cf. equation 5). The longitudinal part of the polarization is neglected in the weak anisotropy approximation assumed here. However, before neglecting the longitudinal part, it is relevant to note that the transformation of a longitudinal polarization gives

$$\kappa_t = \frac{\gamma_s \omega}{\omega' |\mathbf{k}'|} (|\mathbf{k}'| \sin \theta', 0, |\mathbf{k}'| \cos \theta' - \omega' \beta_s / c). \quad (20)$$

For $\gamma_s \gg 1$ the transformed longitudinal polarization vector (20) has comparable longitudinal and transverse parts in the new frame. The weak anisotropy approximation is useful only if the longitudinal part of the polarization is negligible in both frames. Provided this approximation is valid, it leads to a major simplification in transforming the polarization vector.

For the transverse polarization vector \mathbf{t} , the transformation gives

$$\mathbf{t}_t = \frac{1}{n} \left[n' \cos \theta' - \frac{\beta_s (1 - n^2)}{1 - n' \beta_s \cos \theta'}, 0, -n' \sin \theta' \right], \quad (21)$$

and for the transverse polarization vector \mathbf{a} it gives $\mathbf{a}_t = \mathbf{a}$. One may rewrite (21) as

$$\mathbf{t}_t = \frac{1}{n} \left\{ \left[n' - \frac{(1 - n^2) \beta_s \cos \theta'}{1 - n' \beta_s \cos \theta'} \right] \mathbf{t}' - \frac{(1 - n^2) \beta_s \sin \theta'}{1 - n' \beta_s \cos \theta'} \boldsymbol{\kappa}' \right\}, \quad (22)$$

with

$$\boldsymbol{\kappa}' = (\sin \theta', 0, \cos \theta'), \quad \mathbf{t}' = (\cos \theta', 0, -\sin \theta'), \quad (23)$$

and with $\mathbf{a}_t = \mathbf{a}' = (0, 1, 0)$. It follows that the transformed transverse polarization vector is also approximately transverse in the primed frame ($\mathbf{t}_t = \mathbf{t}'$) provided that the weak anisotropy approximation is valid – specifically, provided that one may assume $n' \rightarrow 1$ in (22) (cf. equation 18).

3.4 Axial ratio in the pulsar frame

The polarization vectors (5), with $L_{\pm} \rightarrow 0$, transform into $\mathbf{e}'_{\pm} = (T_{\pm} \mathbf{t}' + i \mathbf{a}') / (T_{\pm}^2 + 1)^{1/2}$. The axial ratio is transformed simply by using the solutions (8) of (7) with the parameter R re-expressed in terms of the variables in the primed frame. One finds (cf. equation 15),

$$R \approx \frac{\Omega_e n^2 \sin^2 \theta'}{\eta \omega' n \gamma_s^3 (1 - n' \beta_s \cos \theta')^2 (n' \cos \theta' - \beta_s)}. \quad (24)$$

Making the approximations $n, n' \approx 1$, $\beta_s \approx 1 - 1/2\gamma_s^2$ and considering only forward propagation, $\theta' < \pi/2$ in the primed frame, (16) gives

$$\begin{aligned}\omega/\omega' &\approx \begin{cases} (1 + \gamma_s^2 \theta'^2)/2\gamma_s & \text{for } \gamma_s^2 \theta'^2 \lesssim 1, \\ 2\gamma_s \sin^2(\theta'/2) & \text{for } \gamma_s^2 \theta'^2 \gtrsim 1, \end{cases} \\ \sin \theta &\approx \begin{cases} 2\gamma_s \theta' / (1 + \gamma_s^2 \theta'^2) & \text{for } \gamma_s^2 \theta'^2 \lesssim 1, \\ 1/\gamma_s \tan(\theta'/2) & \text{for } \gamma_s^2 \theta'^2 \gtrsim 1, \end{cases} \\ \cos \theta &\approx (1 - \gamma_s^2 \theta'^2) / (1 + \gamma_s^2 \theta'^2).\end{aligned}\quad (25)$$

Then (24) reduces to

$$R \approx \frac{\Omega_e}{\eta\omega'} \begin{cases} \frac{8\gamma_s^3\theta'^2}{(1+\gamma_s^2\theta'^2)^2} \frac{1}{1-\gamma_s^2\theta'^2} & \text{for } \gamma_s^2\theta'^2 \lesssim 1, \\ \frac{\cos^2(\theta'/2)}{2\gamma_s^3 \sin^4(\theta'/2)} \frac{1+\gamma_s^2\theta'^2}{1-\gamma_s^2\theta'^2} & \text{for } \gamma_s^2\theta'^2 \gtrsim 1. \end{cases} \quad (26)$$

For semiquantitative purposes, the approximation for $\gamma_s^2\theta'^2 \lesssim 1$ suffices for all angles, $\theta' < \pi/2$, in the forward hemisphere. (The error in using it is about 30 per cent at $\theta' = \pi/2$.)

In interpreting (26), it is useful to consider the transition angles that are the solutions of $|R| = 2$ that define the forward and backward cones of high CP. In the rest frame the forward and backward cones are equal, with θ_c given by (10) or (11). The Lorentz transformation with $\gamma_s \gg 1$ shrinks the forward cone dramatically, specifically to $0 \leq \theta' \ll (\eta\omega'/8\Omega_e\gamma_s^2)^{1/2}$, which is tiny. However, the backward cone is expanded, leading to an effect not previously recognized.

3.5 Aberrated backward circular polarization (ABCP)

The Lorentz transformation expands the backward cone of high CP by a large factor. The expanded cone can even extend into the forward hemisphere, in which case it may become relevant to escaping radiation. The condition for the backward cone of high CP in the rest frame to extend to the forward hemisphere in the pulsar frame may be found by requiring $R \lesssim 2$ for $\theta' = \pi/2$ in (26). This gives

$$\omega' \gtrsim \frac{\Omega_e}{2|\eta|\gamma_s^3}. \quad (27)$$

All radiation at $\theta' > 1/\gamma_s$ has at least a small degree of CP characteristic of backward waves in the rest frame, and when (27) is satisfied, the degree of polarization becomes high, $r_c > 1/\sqrt{2} = 71$ per cent, at an angle $\theta' < \pi/2$. We refer to this effect as aberrated backward circular polarization (ABCP).

One can describe ABCP in terms of contours of fixed r_c in θ' - ω' space (cf. Fig. 4 in Section 4.5). For $|R| \gg 1$ one has $|r_c| \approx 2/|R|$, and the contours are determined by

$$\theta' = 2 \arccos \left[(\xi^2 + 1)^{1/2} - \xi \right], \quad \xi = \frac{r_c}{\omega'} \frac{\Omega_e}{8|\eta|\gamma_s^3}. \quad (28)$$

The condition (27) is more restrictive than necessary: it is a condition for large CP, whereas for most pulsars the CP is relatively weak. One can have small but significant CP at oblique angles, $\theta' \sim 1$, at frequencies much lower than that determined by (27), provided one has $\xi \gtrsim 1$. Specifically, for a given $|r_c| \ll 1$, the condition $\xi \gtrsim 1$ is satisfied for frequencies a factor $\sim |r_c|$ smaller than that determined by (27).

4 INCLUSION OF RELATIVISTIC RANDOM MOTIONS

The theory in the previous two sections ignores the random motions of the particles in the rest frame of the plasma. The spread in Lorentz factors, $\langle \gamma \rangle$, where angular brackets denote an average over the distribution of particles, is thought to be large, with recent estimates (Zhang & Harding 2000; Hibschan & Arons 2001; Arendt & Eilek 2002) suggesting a value $\langle \gamma \rangle \sim 10$ in the rest frame of the plasma, considerably less than the bulk Lorentz factor, $\gamma_s \sim 100$ with which the plasma is streaming. A large relativistic spread implies $\Delta\beta^2 = \langle \gamma \beta^2 \rangle / \langle \gamma \rangle \sim 1$, compared with a non-relativistic spread, $\Delta\beta^2 \ll 1$, and the cold plasma limit, $\Delta\beta^2 \rightarrow 0$.

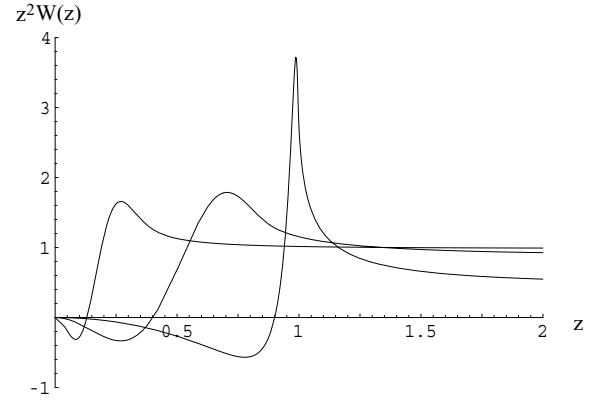


Figure 2. The function $z^2 W(z)$ is plotted for a thermal distribution with thermal energies 0.01 (leftmost), 0.1 (middle) and 1 (rightmost) times the rest energy of the electron. [After Melrose & Gedalin (1999).]

4.1 Approximations to the dielectric tensor

A general expression is available for the dielectric tensor for a pulsar plasma with one-dimensional distributions of electrons and positrons with arbitrary distribution functions. The components of this tensor are written down in the Appendix for frequencies well below the cyclotron resonance. Only one relativistic plasma dispersion function is then involved and it is denoted $W(z) = \langle \gamma^{-3}(z - \beta)^{-2} \rangle$, with $z = \omega/|k|c \cos \theta$ (Gedalin et al. 1998).

The gyrotropic terms in the response tensor determine the ellipticity of the natural modes, and these terms are the 12-, 21-, 23- and 32-components of the response tensor. These components involve the charge density, $\rho = \eta en$, and the current density, \mathbf{J} . Only the terms involving η are retained here. In a more general treatment, one would also need to include a non-zero current density and to take the cyclotron resonance into account. With the simplifying assumptions made here, the only gyrotropic terms are the 12- and 21-components, as in the magneto-ionic (cold plasma) case.

The function $z^2 W(z)$, which appears in the 33-component of the response tensor, characterizes the relativistic dispersion. This function is illustrated in Fig. 2 for a one-dimensional Jüttner (relativistic thermal) distribution, showing how a peak develops just below $z = 1$ and the asymptotic value decreases below unity as the temperature becomes relativistic.

In the weak anisotropy limit one has $z = \sec \theta$, and relativistic effects are characterized by the function $\sec^2 \theta W(\sec \theta)$. This function decreases steeply from a large value, $\langle \gamma \rangle (1 + \Delta\beta^2) \approx 2\langle \gamma \rangle$, at $\theta = 0$ to a small value, $\langle 1/\gamma^3 \rangle \sim 1/\langle \gamma \rangle$, at $\theta = \pi/2$. An interpolation gives

$$\sec^2 \theta W(\sec \theta) = \begin{cases} \frac{2\langle \gamma \rangle}{1 + \theta^4/\theta_0^4} & \text{for } \theta \lesssim \theta_0, \\ \left\langle \frac{1}{\gamma^3} \right\rangle \frac{1 + \cos^2 \theta}{\sin^4 \theta} & \text{for } \theta \gtrsim \theta_0, \end{cases} \quad (29)$$

with $\theta_0^4 = \langle 1/\gamma^3 \rangle / \langle \gamma \rangle \sim 1/\langle \gamma \rangle^2$, implying $\theta_0 \sim 1/\langle \gamma \rangle^{1/2}$. In contrast, in the cold plasma limit, this function is replaced by unity ($\langle \gamma \rangle \rightarrow 1$, $\Delta\beta^2 \rightarrow 0$, $\langle 1/\gamma^3 \rangle \rightarrow 1$).

4.2 Modified magneto-ionic theory

In the frequency range well below the cyclotron frequencies of the relativistic particles, the wave equation is of the form $\Lambda^i_j E^j = 0$,

with Λ^i_j given by

$$\Lambda = \begin{pmatrix} \tilde{S} - \tilde{n}^2 \cos^2 \theta & -i\tilde{D} & \tilde{n}^2 \cos \theta \sin \theta \\ i\tilde{D} & \tilde{S} - \tilde{n}^2 & 0 \\ \tilde{n}^2 \cos \theta \sin \theta & 0 & \tilde{P} - \tilde{n}^2 \sin^2 \theta \end{pmatrix}, \quad (30)$$

with

$$\tilde{S} = 1 + \frac{\tilde{X}}{\tilde{Y}^2}, \quad \tilde{D} = \eta \frac{\tilde{X}}{\tilde{Y}}, \quad \tilde{P} = 1 - \frac{\omega_p^2}{\omega^2} z^2 W(z), \quad (31)$$

with the modified magneto-ionic parameters identified as

$$\tilde{X} = \frac{\omega_p^2}{\langle \gamma \rangle \omega^2}, \quad \tilde{Y} = \frac{\Omega_e}{\langle \gamma \rangle \omega}. \quad (32)$$

The remaining quantity in (30) is

$$\tilde{n}^2 = n^2 \left(1 - \frac{\Delta \beta^2}{\beta_A^2} \right), \quad (33)$$

where β_A^2 is defined in the appendix. Equation (30) is of the same form as the corresponding equation in magneto-ionic theory, which corresponds to omitting the tildes, and with $P = 1 - X$.

The dispersion equation is given by setting the determinant of the matrix (30) to zero, and the polarization vectors are constructed from the matrix of cofactors, as in the magneto-ionic case. The functions L and T that describe the polarization in (5) for each mode are given by

$$L = \frac{(\tilde{P} - \tilde{n}^2)D \sin \theta}{\tilde{A}\tilde{n}^2 - \tilde{P}\tilde{S}}, \quad T = \frac{\tilde{D}\tilde{P} \cos \theta}{\tilde{A}\tilde{n}^2 - \tilde{P}\tilde{S}}, \quad (34)$$

with \tilde{n}^2 interpreted as the solution of the dispersion equation for that mode. As in the magneto-ionic case, the axial ratio T satisfies a quadratic equation, which is

$$T^2 - \frac{(\tilde{P}\tilde{S} - \tilde{S}^2 + \tilde{D}^2) \sin^2 \theta}{\tilde{P}\tilde{D} \cos \theta} T - 1 = 0, \quad (35)$$

and which reduces to (7) in the magneto-ionic limit. Again the axial ratio is determined by a single combination of parameters, denoted by R in (7). The expression (15) for R in a cold plasma is replaced, in a highly relativistic plasma, by

$$R \approx \frac{\Omega_e}{\eta \omega} \frac{\sin^2 \theta}{\cos \theta} \sec^2 \theta W(\sec \theta). \quad (36)$$

The function $\sec^2 \theta W(\sec \theta)$ is approximated by (29) in a highly relativistic plasma, and is replaced by unity in a non-relativistic plasma.

4.3 CP in highly relativistic plasmas

The CP is determined by the parameter R , and the dependence of R on angle can be quite different in the relativistic case compared to the non-relativistic case. In the latter (magneto-ionic) case, R depends on angle through the factor $\sin^2 \theta / \cos \theta$, which increases monotonically with θ from zero at $\theta = 0$ to infinity at $\theta = \pi/2$. In a highly relativistic plasma there is an additional dependence on θ through the function $\sec^2 \theta W(\sec \theta)$ (cf. equation 29). The variation of R with θ then follows from (36) with (29):

$$R \approx \begin{cases} \frac{\Omega_e}{\eta \omega} \frac{2\langle \gamma \rangle \theta^2}{1 + \theta^4 / \theta_0^4} & \text{for } \theta \lesssim \theta_0, \\ \frac{\Omega_e}{\eta \omega} \left\langle \frac{1}{\gamma^3} \right\rangle \frac{1 + \cos^2 \theta}{\cos \theta \sin^2 \theta} & \text{for } \theta \gg \theta_0, \end{cases} \quad (37)$$

with θ_0 defined below (29). There is a rapid increase, $R \propto \theta^2$, to a peak value for $\theta \approx \theta_0$, followed by a decrease to a minimum at

intermediate angles $\theta \sim 1$, as discussed below, and an increase to infinity at $\theta = \pi/2$. The variation for $\pi/2 \leq \theta \leq \pi$ is a mirror image, as a result of R being an odd function of $\cos \theta$.

The value of R for $\sin \theta \ll 1$ is $\approx 2\langle \gamma \rangle$ times its value in a cold plasma. This implies that the forward cone of high CP is much smaller than in the cold plasma case. Specifically, (10) is replaced by

$$\theta_c = (\omega |\eta| / 2\Omega_e \langle \gamma \rangle)^{1/2}. \quad (38)$$

If this were the only change, one would conclude that the inclusion of random relativistic motions reduces the range of angles where the natural modes have significant CP. However, the minimum in R at intermediate angles can allow another range of high CP.

4.4 Intrinsically relativistic circular polarization (IRCP)

Small values of $|R|$ imply large CP, and the decrease of $|R|$ due to relativistic effects allows the possibility of an intrinsically relativistic regime of high CP (IRCP). The minimum of R is determined by the extremum of $(1 + \cos^2 \theta) / \cos \theta \sin^2 \theta$, which occurs at $\cos^2 \theta = \sqrt{5} - 2$, corresponding to $\theta = 61^\circ$ and $(1 + \cos^2 \theta) / \cos \theta \sin^2 \theta = 3.3$. A region of high IRCP is present if the condition

$$\frac{3.3\Omega_e}{|\eta|\omega} \left\langle \frac{1}{\gamma^3} \right\rangle \lesssim 1 \quad (39)$$

is satisfied. For a given mode, IRCP at $\theta < \pi/2$ has the same handedness as the CP at $\theta = 0$, and because R is an odd function of $\cos \theta$, there is an analogous range of IRCP at $\theta > \pi/2$ that has the opposite handedness, and the same handedness as at $\theta = \pi$.

When the condition (39) is satisfied, there are three transition angles in the range $0 < \theta < \pi/2$, rather than the single transition angle in the cold plasma case. There is the regime of high CP at $\theta \ll \theta_c$, with θ_c determined by (38), a regime of approximately linear polarization at larger θ , then the transition to nearly circular over the range of angles where IRCP applies, with the waves becoming linearly polarized again in a small range of angles about $\theta = \pi/2$.

Small but significant degrees of CP are of interest. Consider the conditions for a degree of CP greater than some small value $r_c = 2/|R|$, with $|R| \gg 1$. Then provided that the parameter

$$\alpha = \frac{r_c |\eta| \omega}{2\Omega_e \langle 1/\gamma^3 \rangle} \quad (40)$$

is small, the range of θ over which the natural modes have a degree of CP in excess of r_c is determined by the solutions of the cubic equation $\alpha x(1 - x^2) = 1 + x^2$, with $x = \cos \theta$. It follows that, for sufficiently small α , IRCP causes CP in excess of r_c for

$$(2\alpha)^{1/2} \lesssim \theta \lesssim \pi/2 - \alpha. \quad (41)$$

For α of order unity, one needs to solve the cubic equation to find the range, which shrinks to zero as α approaches 3.3.

4.5 Transformation to the streaming frame

Transformation to the pulsar frame where the plasma is streaming relativistically leads to some relatively cumbersome results, in particular because of the different approximations for $\theta \lesssim \theta_0$, $\pi - \theta_0$ and $\theta_0 \lesssim \theta \lesssim \pi - \theta_0$ in (37). As noted in connection with (26), for semiquantitative purposes it suffices to use the approximations (25) for $\gamma_s \theta' \lesssim 1$ for all $\theta' < \pi/2$, and doing so simplifies the analysis substantially. The angles $\theta = \theta_0$, $\pi - \theta_0$ transform into

$$\theta'_{0+} = \frac{\theta_0}{2\gamma_s}, \quad \theta'_{0-} = \frac{2}{\gamma_s \theta_0}, \quad (42)$$

respectively. Then applying the approximate forms (25) to the upper approximation in (37) for R gives

$$R \approx \begin{cases} \frac{16\Omega_e}{\eta\omega'} \langle \gamma \rangle \gamma_s^3 \theta^2 & \text{for } \theta' \lesssim \theta'_{0+}, \\ \frac{\Omega_e}{\eta\omega'} \langle \gamma \rangle \cos^2(\theta'/2) & \text{for } \theta' \gtrsim \theta'_{0-}, \end{cases} \quad (43)$$

where the interpolation factor $1/(1 + \theta^4/\theta_0^4) \rightarrow 1/\{1 + [\theta'_{0-}/2 \tan(\theta'/2)]^4\}$ is omitted. The approximation (43) includes ABCP, which is similar in form to that in a cold plasma (cf. equation 26), but with $\Omega_e \rightarrow \Omega_e 2\langle \gamma \rangle$. Qualitatively, this implies that for given ω'/Ω_e the modes are less circularly polarized for $\langle \gamma \rangle \gg 1$ than in a cold plasma ($\langle \gamma \rangle \rightarrow 1$).

The lower approximation in (37) applies in the range $\theta'_{0+} \lesssim \theta' \lesssim \theta'_{0-}$, and gives

$$R \approx \frac{\Omega_e}{\eta\omega'} 2\gamma_s \left\langle \frac{1}{\gamma^3} \right\rangle \frac{1 + \gamma_s^4 \theta'^4}{\gamma_s^2 \theta'^2 (1 - \gamma_s^2 \theta'^2)}. \quad (44)$$

The form (44) describes IRCP, which applies either side of the pole at $\theta' = 1/\gamma_s$, with the final factor further approximated by $1/\gamma_s^2 \theta'^2$ for $\gamma_s^2 \theta'^2 \ll 1$ and by -1 for $\gamma_s^2 \theta'^2 \gg 1$. High CP due to IRCP requires $(\Omega_e/|\eta|\omega') 2\gamma_s \langle 1/\gamma^3 \rangle \lesssim 1$, and this is not satisfied under the conditions assumed in this paper. Hence, IRCP can lead to at most a low degree of CP, $r_c \approx 2/|R| \ll 1$.

In Fig. 3 we plot r_c as a function of θ' in the pulsar frame around the value $\theta'\gamma_s = 1$ where r_c passes through zero. (The choice $\omega' = \Omega_e$ in

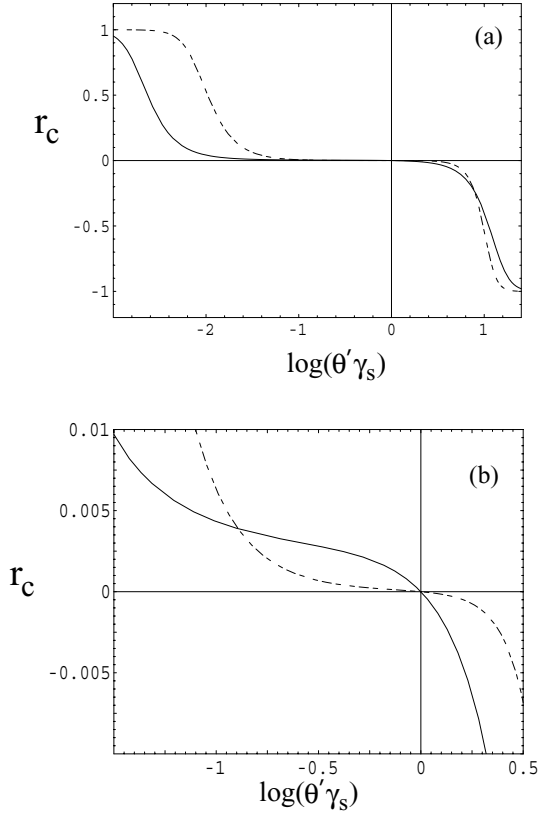


Figure 3. The degree of circular polarization, r_c , is plotted as a function of angle, θ' , in the pulsar frame for a cold plasma (dashed line) and an intrinsically relativistic plasma (solid line). The parameters chosen are: $\Omega_e/\omega'_p = \omega'/\omega'_p = 10^2$, $\gamma_s = 200$, $\eta = 0.1$ and, for the solid line, $\langle \gamma \rangle = 10$. Plot (b) complements (a) by showing the structure near $\theta'\gamma_s = 1$. Note that the far right-hand portion of plot (a), specifically for $\theta'\gamma_s \gtrsim 6$, is inconsistent with the neglect of the cyclotron resonance.

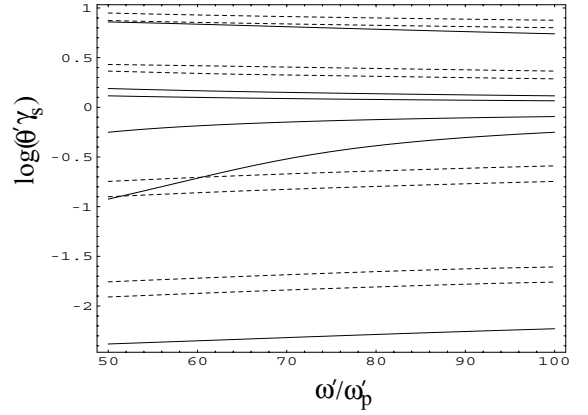


Figure 4. Contour plots for the degree of circular polarization in the ω' - θ' plane in the pulsar frame. Dashed curves are for a cold plasma and solid curves for an intrinsically relativistic plasma, both with the same parameters as in Fig. 3. Contours (dashed lines) from top to bottom: $r_c = -0.2, -0.1, -2 \times 10^{-3}, -10^{-3}, 10^{-3}, 2 \times 10^{-3}, 0.1, 0.2$; contours (solid lines): $r_c = -0.1, -2 \times 10^{-3}, -10^{-3}, 10^{-3}, 2 \times 10^{-3}, 0.1$.

the pulsar frame corresponds to a low frequency, $\omega \approx \Omega_e/\gamma_s$ for the range of θ' shown, and r_c varies only slowly with ω' .) Comparing the solid curve, for an intrinsically relativistic plasma, with the dashed curve, for a cold plasma, one concludes that, owing to intrinsically relativistic effects, the value of $|r_c|$ is enhanced compared to a cold plasma when $|r_c|$ is small, but reduced compared to a cold plasma for larger values of $|r_c|$. There is an asymmetry such that $|r_c|$ is larger over a wider range of angles at $\theta'\gamma_s < 1$ than at $\theta'\gamma_s > 1$. For the parameters chosen, IRCP cannot be large; nevertheless, the inclusion of intrinsically relativistic effects (solid curves) causes a large increase, compared to a cold plasma (dashed curves), in the value of CP either side of the angle $\theta' = 1/\gamma_s$ at which it passes through zero.

In Fig. 4 we show contour plots for r_c as a function of ω' and θ' ; the intersections with the line $\omega'/\omega'_p = 100$ correspond to the values implied by Fig. 2, and the contour plot shows the weak dependence on ω' for lower frequencies.

5 ORIGIN OF THE OBSERVED CIRCULAR POLARIZATION

Any explanation of the CP based on elliptically polarized OMs should allow for the wide range of properties of the CP observed: low CP in most pulsars at most phases, moderate CP only at some specific phases in some pulsars (Karastergiou et al. 2001, 2002), the possibility that the CP can have either handedness at specific phases (Karastergiou et al. 2003b), and a tendency for higher CP at higher frequencies (von Hoensbroech & Lesch 1999). In principle the relativistic effects discussed here appear capable of accounting for the observed features, provided that the observed polarization is characteristic of a polarization limiting region sufficiently far from the surface of the star.

5.1 Effects of ABCP

In ABCP, a region of high CP in a small backward cone in the rest frame of the plasma expands, as a result of aberration, to fill a large fraction of the 4π steradians. The condition (26) for this to occur in a cold plasma is modified in an intrinsically relativistic plasma by inclusion of an additional factor $2\langle \gamma \rangle$ in (43). The requirement for a

degree of circular polarization $r_c = 2/|R| \ll 1$ at frequency ω' and (forward) angle θ' becomes

$$r_c \approx \frac{|\eta|\omega'}{\Omega_e} \frac{2\gamma_s^3 \sin^4(\theta'/2)}{\langle \gamma \rangle \cos^2(\theta'/2)}. \quad (45)$$

For relatively large angles of propagation, (45) implies $r_c \approx |\eta|\omega'/\Omega_e$. An implication is that the degree of CP should increase linearly with frequency due to ABCP. The increase in CP at high frequencies observed in some pulsars (von Hoensbroech & Lesch 1999) is consistent with this prediction.

5.2 Effects of IRCP

The condition for IRCP to lead to high CP is given by setting $|R| = 2$ in (44), but as already noted this requires a frequency that is too high to be consistent with our assumptions. However, IRCP can account for a small degree of CP. On writing the condition for a small r_c in the same form as (45), then (44) implies

$$r_c \approx \frac{|\eta|\omega'}{\Omega_e} \frac{1}{\gamma_s \langle (1/\gamma^3) \rangle}, \quad (46)$$

at angles $\gamma_s \theta'$ greater than but of order unity. The range of angles over which IRCP is possible is limited by the requirement $\theta' \ll \theta'_{0-}$, implying that IRCP is confined to a small range of angles around $\theta' \sim 1/\gamma_s$.

Qualitatively, IRCP appears to provide a plausible explanation for observed random changes in handedness from pulse to pulse at a fixed phase in some pulsars. Specifically, IRCP allows the possibility of changes in handedness with small changes in angle near $\gamma_s \theta' = 1$ for waves in a specific mode. For $\gamma_s \sim 100$ this change occurs at $\theta' = 0.01 = 0.5^\circ$. Quantitatively, the condition (46) is satisfied only at frequencies that seem implausibly high for propagation effects to be important, and the angle $\theta' = 1/\gamma_s$ at which the change in handedness occurs seems implausibly small for radiation far from the source region.

The fact that IRCP provides such a natural qualitative explanation for the observed random changes in handedness, suggests that ways in which these quantitative difficulties might be overcome should be explored. The high frequency at which the phenomenon occurs may be modified substantially by inclusion of the effects of the cyclotron resonance; we are currently exploring the required generalization of theory needed to discuss this effect in detail. The difficulty with the smallness of $\theta' = 1/\gamma_s$ may be overcome if the Lorentz factor γ_s is smaller (at least in the polarization limiting region) than generally thought. For example, for $\gamma_s \sim 10$, the angle at which the rapid reversal in handedness occurs is $\sim 9^\circ$.

6 CONCLUSIONS

The results obtained in this paper concern the degree of circular polarization (CP) of the natural wave modes of a pulsar plasma at frequencies well below the cyclotron frequency, Ω_e . We identify one relativistic effect (ABCP) that allows significant CP in ways that have not been previously recognized. ABCP arises from the cone of relatively high CP for nearly antiparallel propagation, $\theta \approx \pi$, in the rest frame of the plasma being transformed (aberrated) into the forward hemisphere, $\theta' < \pi/2$, in the pulsar frame. According to (45), the degree of ABCP should increase linearly with frequency, ω' , which is qualitatively consistent with higher CP at higher frequencies in pulsars.

A second intrinsically relativistic mechanism (IRCP) is also identified, which is due to dispersion in an intrinsically relativistic

plasma. Qualitatively, IRCP can account for changes in handedness with small changes in angle about $\theta' = 1/\gamma_s$. This seems to offer a plausible explanation for the observed random changes in the sign of V from pulse to pulse in some pulsars. However, IRCP is possible only at frequencies higher than are consistent with the assumptions made here. The analysis in this paper is currently being extended to include the effects of the cyclotron resonance on the wave dispersion. Such an extension is required to determine the viability of IRCP as an explanation of observed random changes in handedness of the CP.

Our results provide support for the interpretation of CP in pulsars as a propagation effect, in which the polarization is determined at a polarization limiting region far from the point of emission. However, there are a number of important questions that need to be answered before this suggestion can be converted into a realistic model. These include the way the radiation is split into two modes, and the location of the polarization limiting region.

ACKNOWLEDGMENT

We thank Simon Johnston and Aris Karastergiou for helpful discussions and comments.

REFERENCES

- Allen M. C., Melrose D. B., 1982, *Proc. Astron. Soc. Australia*, 4, 365
 Arendt P. N., Jr, Eilek J. A., 2002, *ApJ*, 581, 451
 Arons J., Barnard J. J., 1986, *ApJ*, 302, 120
 Asseo E., Riazuelo A., 2000, *MNRAS*, 318, 983
 Barnard J. J., Arons J., 1986, *ApJ*, 302, 138
 Budden K. G., 1961, *Radio Waves in the Ionosphere*. Cambridge Univ. Press, Cambridge
 Clark R. R., Smith F. G., 1969, *Nat*, 221, 724
 Ekers R. T., Moffat A. T., 1968, *Nat*, 220, 756
 Gedalin M., Melrose D. B., Gruman E., 1998, *Phys. Rev. E*, 57, 3399
 Graham-Smith F., 2003, *Rep. Prog. Phys.*, 66, 173
 Han J. L., Manchester R. N., Xu R. X., Qiao G. J., 1998, *MNRAS*, 300, 373
 Hibschan J. A., Arons J., 2001, *ApJ*, 560, 871
 Karastergiou A. et al., 2001, *A&A*, 379, 270
 Karastergiou A., Kramer M., Johnston S., Lyne A. G., Bhat N. D. R., Gupta Y., 2002, *A&A*, 391, 247
 Karastergiou A., Johnston S., Kramer M., 2003a, *A&A*, 404, 325
 Karastergiou A., Johnston S., Mitra D., van Leeuwen A. G. J., Edwards R. T., 2003b, *MNRAS*, 344, L69
 Kennett M. P., Melrose D. B., Luo Q., 2000, *J. Plasma Phys.*, 64, 333
 Lominadze D. G., Machabeli G. Z., Melikidze G. I., Pataraya, A. D., 1986, *Sov. J. Plasma Phys.*, 12, 712
 Lyne A. G., Smith F. G., Graham D. A., 1971, *MNRAS*, 153, 337
 Lyubarskii Yu. E., Petrova S. A., 1998, *A&A*, 337, 433
 Lyutikov M., 1998, *MNRAS*, 293, 447
 Lyutikov M., Blandford R. D., Machabeli G., 1999, *MNRAS*, 305, 338
 McKinnon M. M., Stinebring D. R., 2000, *ApJ*, 529, 433
 Melrose D. B., 1980, *Plasma Astrophysics, Vol. I, Emission, Absorption and Transfer of Waves in Plasmas*. Gordon & Breach, New York
 Melrose D. B., 1986, *Instabilities in Space and Laboratory Plasmas*. Cambridge Univ. Press, Cambridge
 Melrose D. B., Gedalin M. E., 1999, *ApJ*, 521, 351
 Melrose D. B., McPhedron R. C., 1991, *Electromagnetic Processes in Dispersive Media*. Cambridge Univ. Press, Cambridge
 Melrose D. B., Stoneham R. J., 1977, *Proc. ASA*, 3, 120
 Melrose D. B., Gedalin M. E., Kennett M. P., Fletcher C. S., 1999, *J. Plasma Phys.*, 62, 233
 Petrova S. A., 2001, *A&A*, 378, 883
 Radhakrishnan V., Rankin J. M., 1990, *ApJ*, 352, 528

- Sazonov V. N. Tsytovich V. N., 1968, Radiophys. Quantum Electron., 11, 731
- Stinebring D. R., Cordes J. M., Rankin J. M., Weisberg J. M., Boriakoff V., 1984, ApJS, 55, 247
- Stix T. H., 1962, The Theory of Plasma Waves. McGraw-Hill, New York
- Sturrock P. A., 1971, ApJ, 164, 529
- Volokitin A. S., Krasnoselskikh V. V., Machabeli G. Z., 1985, Sov. J. Plasma Phys., 11, 531
- von Hoensbroech A., Lesch H., 1999, A&A, 342, L61
- Zhang B., Harding A. K., 2000, ApJ, 532, 1150

APPENDIX A: MODIFIED COLD PLASMA MODEL

For a non-gyrotropic pulsar plasma, the dielectric tensor can be written as (e.g. Melrose & Gedalin 1999; Melrose et al. 1999; Kennett et al. 2000). For frequency low compared with the actual cyclotron frequencies in the relativistic plasma, the space components of the response 4-tensor for one species of particle, with charge $q = \eta|q|$, mass m and number density n , reduce to

$$\alpha^{11} = \alpha^{22} = -\frac{q^2 n}{m} \frac{k_{\parallel}^2 c^2}{\Omega_e^2} (z^2 \langle \gamma \rangle - 2z \langle \gamma \beta \rangle + \langle \gamma \beta^2 \rangle),$$

$$\alpha^{33} = \frac{q^2 n}{m} \left[z^2 W(z) + \frac{k_{\perp}^2 c^2}{\Omega_e^2} \langle \gamma \beta^2 \rangle \right],$$

$$\alpha^{12} = -\alpha^{21} = -i\eta \frac{q^2 n}{m} \frac{k_{\parallel} c}{\Omega_e} (z - \langle \beta \rangle),$$

$$\alpha^{13} = \frac{q^2 n}{m} \frac{k_{\perp} k_{\parallel} c^2}{\Omega_e^2} (z \langle \gamma \beta \rangle - \langle \gamma \beta^2 \rangle),$$

$$\alpha^{23} = -\alpha^{32} = i\eta \frac{q^2 n}{m} \frac{k_{\perp} c}{\Omega_e} \langle \beta \rangle, \quad (\text{A1})$$

with $z = \omega/k_{\parallel}c$ and with $\mathbf{k} = (k_{\perp}, 0, k_{\parallel})$. The average is over the one-dimensional particle distribution, with the relativistic plasma dispersion function defined by

$$W(z) = \left\langle \frac{1}{\gamma^3(z - \beta)^2} \right\rangle = \int_{-\infty}^{\infty} \frac{dp}{\beta - z} \frac{df(p)}{dp}, \quad (\text{A2})$$

where $f(p)$ is the one-dimensional distribution function, normalized by $\int dp f(p) = 1$. Other parameters in (A1) may be written in terms of the plasma frequency, $\omega_p = (e^2 n / \epsilon_0 m)^{1/2}$, and

$$\beta_A = \langle \gamma \rangle^{-1/2} \frac{\Omega_e}{\omega_p}, \quad \langle \gamma \beta^2 \rangle = \langle \gamma \rangle \Delta \beta^2, \quad (\text{A3})$$

where $\beta_A c$ is the Alfvén speed in the pair plasma. The parameter $\Delta \beta^2 c^2$ is the mean square speed in a non-relativistic plasma, where one has $\Delta \beta^2 = \langle v^2 \rangle / c^2 \ll 1$, and an intrinsically highly relativistic plasma is characterized by $\Delta \beta^2 \rightarrow 1$.

The result used in Section 2 is for the dielectric tensor in the rest frame of the plasma. The components of the dielectric tensor, $K^i_j = \delta^i_j - \alpha^i_j / \epsilon_0 \omega^2$, where δ^i_j is the unit tensor, and where the mixed components, α^i_j , are numerically equal to minus the contravariant components, α^{ij} , given by (A1). The rest frame corresponds to the frame in which the bulk momentum is zero, $\langle \gamma \beta \rangle = 0$, and all averages that involve odd powers of β are neglected in Section 2.

This paper has been typeset from a $\text{\TeX}/\text{\LaTeX}$ file prepared by the author.